Laser-induced breakdown spectroscopy analysis of copper and nickel in chelating resins for metal recovery in wastewater

Marina Martínez-Minchero, Laura Ulloa, Adolfo Cobo, Eugenio Bringas, Mª-Fresnedo San-Román, José Miguel López-Higuera

PII: S0584-8547(21)00124-5

DOI: https://doi.org/10.1016/j.sab.2021.106170

Reference: SAB 106170

To appear in: *Spectrochimica Acta Part B: Atomic Spectroscopy*

Received date: 1 September 2020

Revised date: 5 March 2021

Accepted date: 8 March 2021

Please cite this article as: M. Martínez-Minchero, L. Ulloa, A. Cobo, et al., Laser-induced breakdown spectroscopy analysis of copper and nickel in chelating resins for metal recovery in wastewater, *Spectrochimica Acta Part B: Atomic Spectroscopy* (2021), https://doi.org/10.1016/j.sab.2021.106170

Laser-Induced Breakdown Spectroscopy analysis of copper and nickel in chelating resins for metal recovery in wastewater

Marina Martínez-Minchero[a,b], Laura Ulloa[c], Adolfo Cobo[a,d] Eugenio Bringas[c], Mª-Fresnedo San-Román[c] and José Miguel López-Higuera[a,b,d]

[a]Photonics Engineering Group, Department of TEISA, Universidad de Cantabria, Avda. De los Castros, 39005, Santander, Spain

[b]Instituto de Investigación Sanitaria Valdecilla (IDIVAL), 39005 Cantabria, Spain

[c]Dept. Ingenierías Química y Biomolecular, ETSIIyT, Universidad de Cantabria, Avda. Los Castros s/n, 39005 Santander, Spain

[d]CIBER-bbn, Instituto de Salud Carlos III, 28029 Madrid, Spain

Abstract

Recovery of heavy metals from industrial waste streams is becoming an important challenge due to increasing wastewater production. Chelating resins provide an effective treatment for selective adsorption of metals. Several analytical techniques can be used to assess the adsorption performance, but LIBS offers the unique advantage of in-process continuous monitoring. In this work, LIBS measurements of copper and nickel spectra were performed on single and bi-component resin samples. Single component calibration curves for copper and nickel were obtained with high correlation (R^2=0.99 and R^2=0.98 respectively). Bi-component resin measurements reveal good prediction accuracy for nickel and copper concentrations, the mean relative error in

concentration prediction being 4.69% and 7.98% respectively. From the calibration curves, the prediction of concentration shows a high correlation with the real values (R^2 = 0.99 for copper and 0.98 for nickel).

Keywords

LIBS, Spectroscopy, Chelating resins, Adsorption, Heavy metals, Metal recovery, Wastewater.

1. Introduction

With the rapid development of modern industry and agriculture, waste treatment has been an important issue to take into account. A huge quantity of industrial wastewaters contaminated with toxic compounds like heavy metals are generated and discharged every year by metallurgy and electroplating industries, mining, pesticide manufacturing, etc.[1,2,3] Recovery of valuable compounds from industrial wastes provides economic and environmental benefits, in particular, the selective recovery of metals from wastewaters is an important strategy to minimize raw material and natural resource consumption, as well as to avoid environmental contamination. One common type of industrial wastewater is spent acid solutions, considered hazardous wastes due to the presence of high concentrations of acids and transition metals, such as nickel and copper. The selective recovery of target metals is complicated in most of cases because the metals are dissolved together with large amounts of iron in different concentration levels. The main treatment technologies that have been used in metal content reduction from industrial waste include membrane processes[4,5,6], electrolytic methods[7,8], solvent extraction[9], chemical precipitation[10], ion exchange[11] and adsorption[12–15]. Chemical precipitation has traditionally been the most used method, but it produces considerable

amounts of toxic solid residues that would finally be disposed of as hazardous wastes in landfills with high related costs[16]. Recently, adsorption methods have received considerable attention and the development of high-performance adsorbents for removing heavy metal ions from wastewater is considered a research priority in the environmental field[2,17]. Polymer-based ion exchange resins constitute a well-established, environmentally friendly technology that has found increasing application over the last decade given its high selectivity, lack of sludge production and the recovery of valuable metals. Moreover, ion exchange resins are available commercially[18,19] for almost any separation process. In hydrometallurgy, ion exchange technology is applied in wastewater treatment, in uranium recovery, in separation the platinum group metals, and in removing impurities like Cu^{2+}, Ni^{2+} and Zn^{2+} from different industrial solutions[20]. Chelating ion exchangers are a subgroup or ion exchange resins. These resins are microporous organic materials composed of coordinating copolymers that have been developed especially for transition metal separation as their functional groups consist of one or more donor atoms such as nitrogen, sulphur, and oxygen (Lewis base) and act as ligands in the presence of certain types of cations (Lewis acids)[19,21,22]. The functional groups contained in the polymeric structure provide the properties of selectivity and adsorption capacity that are the most important characteristics of chelating resins [23]. These resins display a wide range of selectivity values towards transition metals, which depend on the different stabilities of metal complexes at the required pH conditions[2]. Typically, chelating exchange resins facilitate increased adsorption rates, efficiencies, and surface areas when compared to ion exchange resins[24], thus, chelating resin treatment is one of the most effective and attractive methods due to the simplicity of design and ease of operation[25].

Monitoring dynamic changes in the composition of elements adsorbed by chelating resins could be interesting for continuous waste treatment processes. Many spectroscopy techniques can be used for elemental analysis in solid samples; however, time-consuming sample preparation is usually required. Therefore, a real-time analysis technique would be an appropriate solution for monitoring chelating resin adsorption.

Laser-induced breakdown spectroscopy (LIBS) is an atomic emission spectroscopy used for quantitative or qualitative elemental analysis[26], based on spectral analysis of the radiation emitted by plasma generated with the material ablated from the target[27]. Since each element has a unique emission spectrum, the elements present in the sample can be identified by their "chemical fingerprints". The LIBS technique is characterized by its multiple advantages. It is versatile, non-contact and practically non-destructive, but the biggest advantage of LIBS is its ability to analyse in almost real-time any type of material with minimal sample preparation. The number of fields in which LIBS can be applied is increasing every year and there are also major applications for which the analytical features of LIBS seem to fit the requirements perfectly. These fields include industry-oriented analysis, mining, archaeological and cultural-heritage applications, applications under extreme conditions (submarine measurements, spatial missions on Mars, etc.), biological and biomedical subjects, environmental sciences, etc.[28]

In previous work, nickel and copper qualitative LIBS analysis was carried out in chelating resins[29]. In this study, the LIBS technique is applied to chelating resins for metallic adsorption, to verify the feasibility of measuring copper and nickel concentration in environmental applications for wastewater treatments. The ability of LIBS to estimate the concentration of target metals in the chelating resins will be useful

for further in-process dynamic studies of copper and nickel recovery in spent sulphuric acids solutions.

2. Materials and methods

2.1. Materials and sample preparation

The different experiments performed with synthetic solutions were prepared by dissolving $NiSO_4 \cdot 6H_2O$ (Scharlab, S.L., Barcelona (Spain)) $CuSO_4 \cdot 5H_2O$ (Panreac, Barcelona (Spain)) in deionized water, to simulate the composition of spent acids in terms of nickel and copper (average composition in Table 1). When needed, the initial pH of the solution was adjusted using sodium hydroxide 5 mol/L (≥ 97%, Panreac) and sulfuric acid (95-98%, Panreac). All reagents used were analytical grade.

Table 1. Average composition of the sulphuric-based spent acids

Ion	Concentration (ppm)
Al^{+3}	544.5
Cr^{+6}	380.3
Mn^{+2}	64.9
Ni^{+2}	6564
Cu^{+2}	3367
Zn^{+2}	384.4
Cd^{+2}	< 10
Sn^{+2}	< 10
Sb^{+2}	306.7
Pb^{+2}	59.8
Fe^{+2}	22450
SO_4^{-2}	159300
Cl^-	4329
NH_4^+	1880

The chelating resin used in this work was Purolite™ MTS9600 (Figure 1) functionalized with bis-picolylamine group (Bis-PMA)[30] that can form coordinate bonds with most of the toxic metal ions via Lewis acid-base interactions. It consists of polystyrene crosslinked with divinylbenzene with particle sizes in the range between 425 and 1000 μm and particle density 800 g/L. It is a highly selective resin for transition metals such as nickel, cobalt and copper even at low pH, making it appropriate for removal of these elements from solutions with high metallic content[19,31]. Specifically, this commercial resin was confirmed to be an effective adsorbent for the removal of nickel and copper, reaching removal percentages of ≈99% and ≈80% respectively[2].

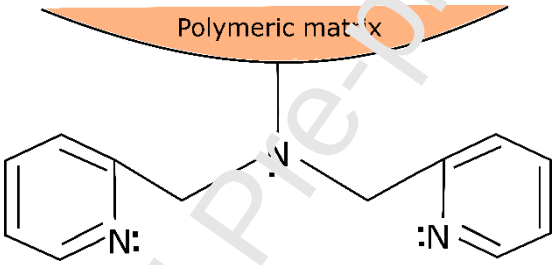

Figure 1. Bis-PMA chemical structure.

Using synthetic solutions, the nickel and copper adsorption performance of the chelating resin Purolite™ MTS9600 was evaluated by contact during 3 h (time needed to reach equilibrium conditions) 5 grams of resin per 12.5 mL of liquid phase. The initial pH of the experiments performed was adjusted to 2.0. Once equilibrium was reached, the solution and the resin were separated and the supernatant liquid characterized in terms of metal concentration using a microwave plasma atomic emission spectroscopy instrument 4210 MP-AES (Agilent Technologies, Santa Clara, Ca, USA). After obtaining the concentration of nickel and copper in the liquid phase, the solid phase concentration was calculated performing a mass balance. The solid phase, i.e., the resin particles, was dried with blotting paper and a hot air stream to ensure moisture removal, and then placed on a plastic slide with double-sided adhesive

tape. After gluing the resin particles, the samples were ready for later measurement with the LIBS setup.

2.2. Experimental setup

The LIBS setup basically comprises a pulsed laser source to ablate the sample and a spectrometer to collect and analyse the atomic emission spectra from the plasma. The laser source is a double-pulsed Nd:YAG (Lotis LS-2134D) operating at a wavelength of 1064 nm with a 10 Hz repetition rate. Due to the physical characteristics of the samples (small and spherical particles shown in Figure 2), the experimental conditions in terms of laser energy have been carefully chosen. An excess of laser energy could easily destroy the resin particles after a single laser shot [...] it was set to 40 mJ of energy per pulse with a pulse width of 16 ns. The measured irradiance on the sample surface was 7.96 GW/cm^2.

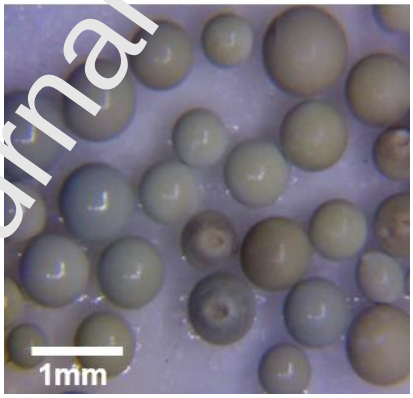

Figure 2. Microscopic image of chelating resin loaded with copper and nickel

The laser beam was focused on the sample with a 75 mm fused-silica focal lens. The spot diameter of the focused laser beam was 200 μm. The light emitted from the plasma generated on the sample surface was captured by a collimating lens and conducted to the spectrometer through a set of two optical fibres. One was a fused silica, solarization resistant, optical fibre with 1mm core diameter, coupled to a another, which was made

up of a bundle of eight optical fibres, each one with a 200 micron core diameter, and a total diameter for the bundle of around 800 microns. The spectrometer used in this study is an eight-channel Avantes ULS2048-USB2-RM spectrometer. The spectral range is from 178 to 889 nm with variable resolution (from 0.015 nm to 0.06 nm) depending on the channel and wavelength.

The setup is fully automated with an XYZ positioner, through-lense imaging and an autofocus system based on image processing. A moving platform was used to obtain measurements of different resin spheres in the sample and to check that the top surface of the resin sphere was focused exactly at the focal point of the LIBS system (Figure 3).

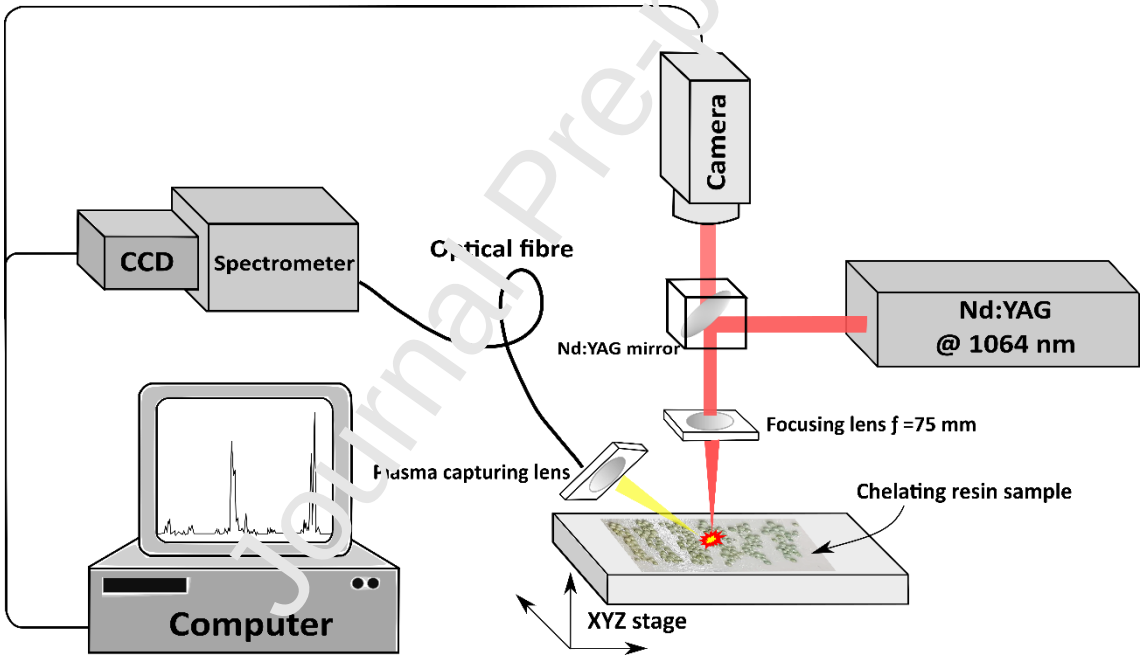

Figure 3. Schematic diagram of the LIBS experimental setup.

In this experiment, the capture delay was set several microseconds before the laser pulse in order to ensure that the plasma emission was captured from the beginning of its formation. The integration time was 1ms (minimum capture window for this spectrometer). With this configuration, the entire duration of the plasma emission was captured, leading to a more stable measurement. The spectra were taken in 10 different

particles of each resin sample, averaging 17 consecutive laser pulses per particle. Every sample was measured twice.

For quantitative analysis, a calibration curve should be obtained in order to relate the measured spectral line intensities to the concentration of the elements of interest in the samples, in this case, copper and nickel. The peak intensities were normalized against a matrix element from the polymeric resin. In these experiments, the peak of Carbon at 247.8nm (C I) was chosen for normalization, as a consequence, the ratio Cu/C and Ni/C was chosen for quantification.

3. Results and discussion

Spectra for both copper and nickel-loaded (after exposure to acid solutions) resins were collected in order to select lines for further calculations. Resins loaded with copper showed a small number of copper peaks in their spectrum, as well as carbon, oxygen and nitrogen peaks from the resin matrix composition. In nickel-loaded resin spectra, several nickel peaks appeared at the same time as resin peaks. The sensitive lines for the aforementioned elements were identified using standard data published by NIST for elemental analysis. Copper (Cu I) line 521.8 nm and nickel (Ni I) line 352.4 nm were selected for quantification. Carbon (C I) line at 247.8 nm was selected for normalization. Figure 4 shows the selected lines in the resin spectra.

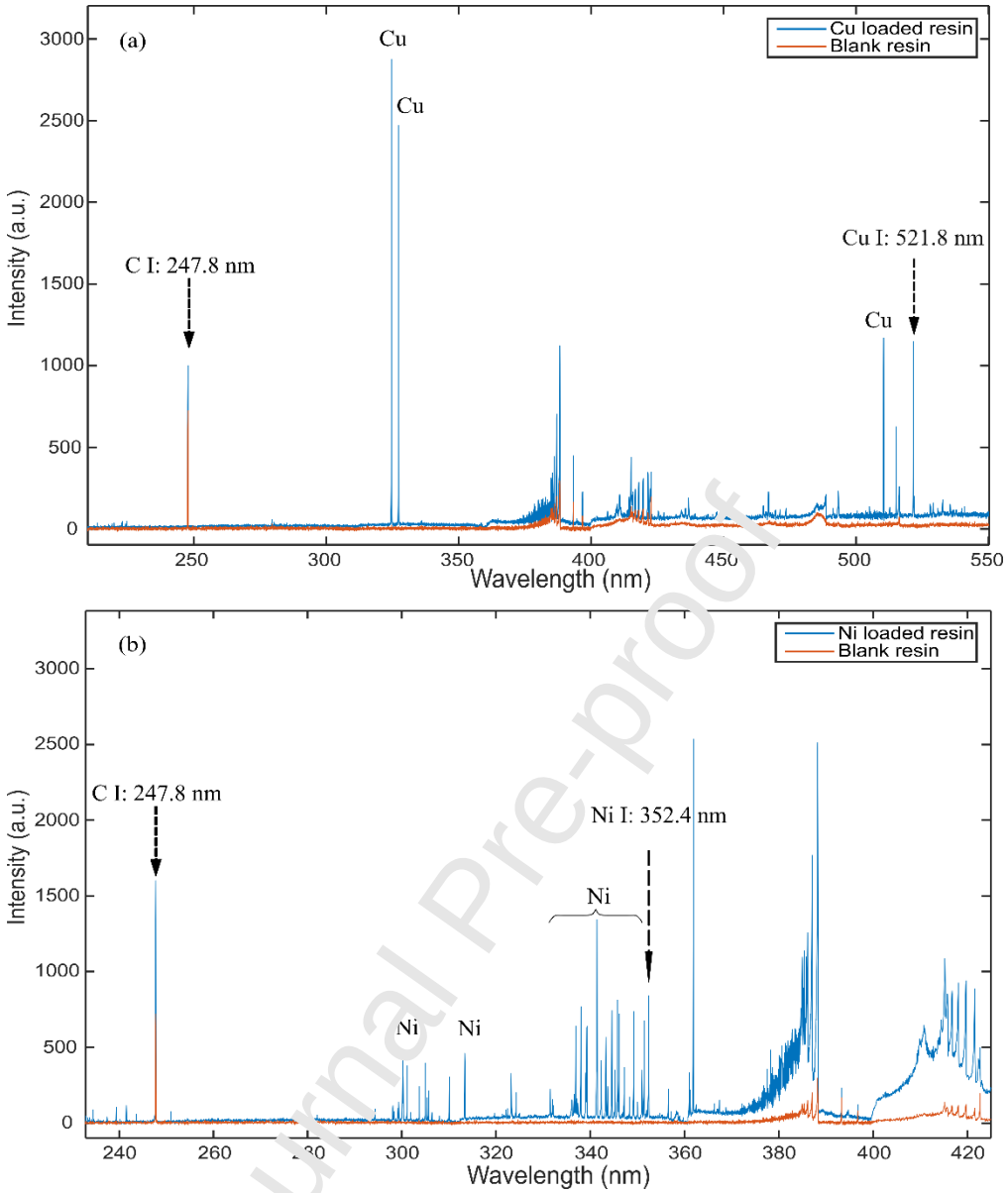

Figure 4. The raw LIBS spectra of blank resin and (a) resin particle loaded with Cu and (b) resin loaded with Ni and the peaks selected for quantification.

To calculate the intensity ratios between the metal and the carbon peaks, the integrated area (background subtracted) of the emission peaks was used to obtain the ratios.

3.1. Calibration curve for copper and nickel

LIBS spectra of different Cu and Ni resin samples were recorded in order to calculate the integrated intensity values of the selected elemental lines. Calibration curves were

obtained by relating the intensity ratios among the metallic element peaks and the matrix carbon peak with the sample concentrations. A fitted calibration curve will enable prediction of Cu and Ni concentration of unknown samples. In Table 2, the concentrations of each measured sample are shown.

Table 2. Samples for calibration curves

Sample	$CuSO_4$ concentration (g/L)	Cu in resin (g Cu/ kg dry resin)	Sample	$NiSO_4$ concentration (g/L)	Ni in resin (g Ni/ kg dry resin)
1	0.5	2.78	**1**	1	5.56
2	1	5.56	**2**	3	16.67
3	1.5	8.33	**3**	5	27.78
4	2	11.11	**4**	7	38.89
5	2.5	13.89	**5**	9	40.4
6	3	16.67	**6**	11	44.35
7	7.5	42.03	**7**	20	63.28
8	8	43.94			
9	10	52.62			
10	12	62.22			

Two different calibration curves, one for each metal, were obtained. For each concentration, the ratio 352.4 nm/247.8 nm for Ni, and 521.8 nm/247.8 nm for copper, were calculated, and the resulting calibration curves are shown in Figure 5. Limit of detection (LOD) was calculated for both elements according to equation 1.[32]

$$LOD = \frac{3\,s_B}{b} \quad (1)$$

Where s_B is the standard deviation of the background and b is the is the magnitude of the slope associated with the linear part of the calibration curve.

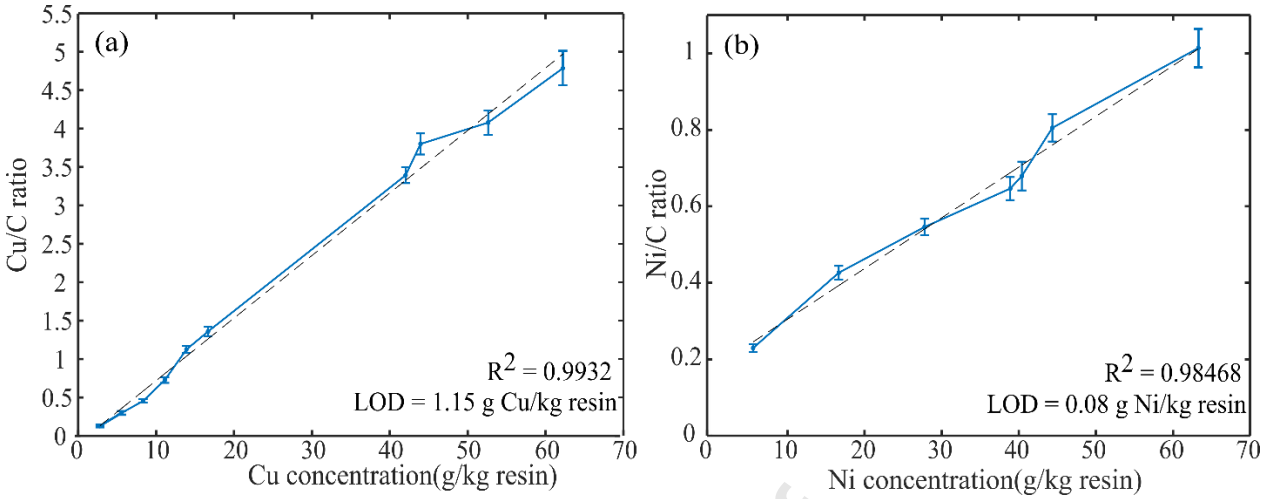

Figure 5. Calibration curves for copper (a) and nickel (b). Error bars represent standard error of the mean (SEM). From the calibration curves, the limit of detection (LoD) has been calculated for both copper and nickel. RSD for both experiments has a similar value of 15.5%.

The R^2 values for the Cu and Ni calibration curves were 0.993 and 0.985 respectively. These curves show a good linear relationship between the LIBS signal and the actual value of Cu concentration, being a little lower for Ni. These results show the suitability of these calibration curves for the measurement of concentrations of one-component samples.

3.2. Bi-component samples

In order to observe how the intensities of copper and nickel peaks are influenced by the presence of the other element (i.e. matrix effects), mixed resins samples with both metals were prepared . For this purpose, 5 samples were prepared by varying Cu concentration with a constant Ni concentration, and, on the other hand, Cu concentration was fixed while Ni concentration was varied. In Table 3 and Table 4, the concentrations of the mixed solutions of copper and nickel in each experimental set of resin samples are described.

Table 3. Concentration of bi-component samples to study the influence of nickel presence on copper measurements. Nickel concentration set at 22.22 g/kg resin.

Sample	CuSO4 concentration (g/L)	NiSO4 concentration (g/L)	Cu in resin (g Cu/ kg dry resin)	Ni in resin (g Ni/ kg dry resin)
1	2	4	11.11	22.22
2	3	4	16.67	22.22
3	4	4	22.22	22.22
4	5	4	27.78	22.22
5	6	4	33.33	22.22

Table 4. Concentration of bi-component samples to study the influence of copper presence in nickel measurements. Copper concentration set at 22.22 g/kg resin.

Sample	CuSO4 concentration (g/L)	NiSO4 concentration (g/L)	Cu in resin (g Cu/ kg dry resin)	Ni in resin (g Ni/ kg dry resin)
1	4	2	22.22	11.11
2	4	3	22.22	16.67
3	4	4	22.22	22.22
4	4	5	22.22	27.78
5	4	6	22.22	33.33

The evolution of the copper intensity ratio with the real copper concentration can be observed in the presence of a constant nickel concentration of 22.22 g/kg dry resin. In Figure 6a, this relation is clearly linear with a regression coefficient of 0.98. The presence of nickel in the resin sample does not affect the linear correlation between copper concentration and the intensity ratio of Cu/C, as expected.

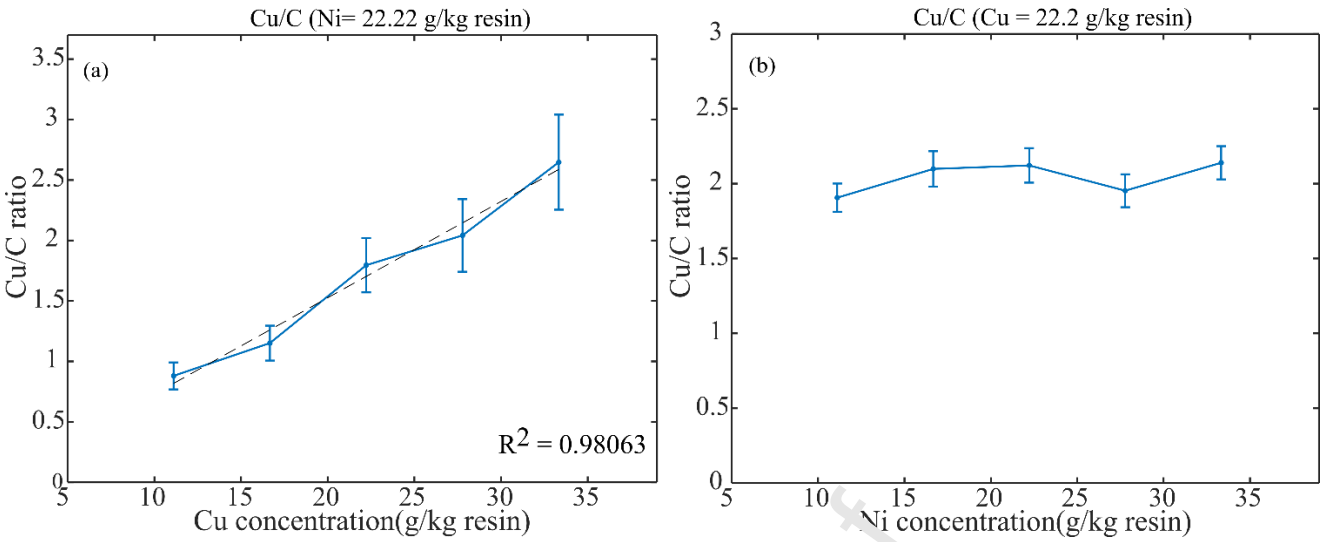

Figure 6. Relation between intensity of Cu/C ratio and Cu concentration while Ni concentration is fixed (a), when Cu concentration is fixed and Ni is increasing (b). Error bars represent standard error of the mean (SEM). The mean RSD of the measurements was 47.8% (a) and 18.1% (b)

On the other hand, when Cu concentration is constant at 22.22 g/kg resin, it can be seen that the ratio intensity of copper is not affected by the growing presence of nickel. The Cu/C ratio is supposed to be constant at a constant copper concentration. This trend is exhibited in figure 6b, which shows Cu/C ratios with small variation due to the intrinsic LIBS fluctuation.

In the case of nickel concentration estimation for a fixed copper concentration, it can be observed that the nickel ratio is linearly dependent on the real Ni concentration. In Figure 7a, the Ni/C ratio increases when nickel concentration increases with a regression coefficient of 0.97.

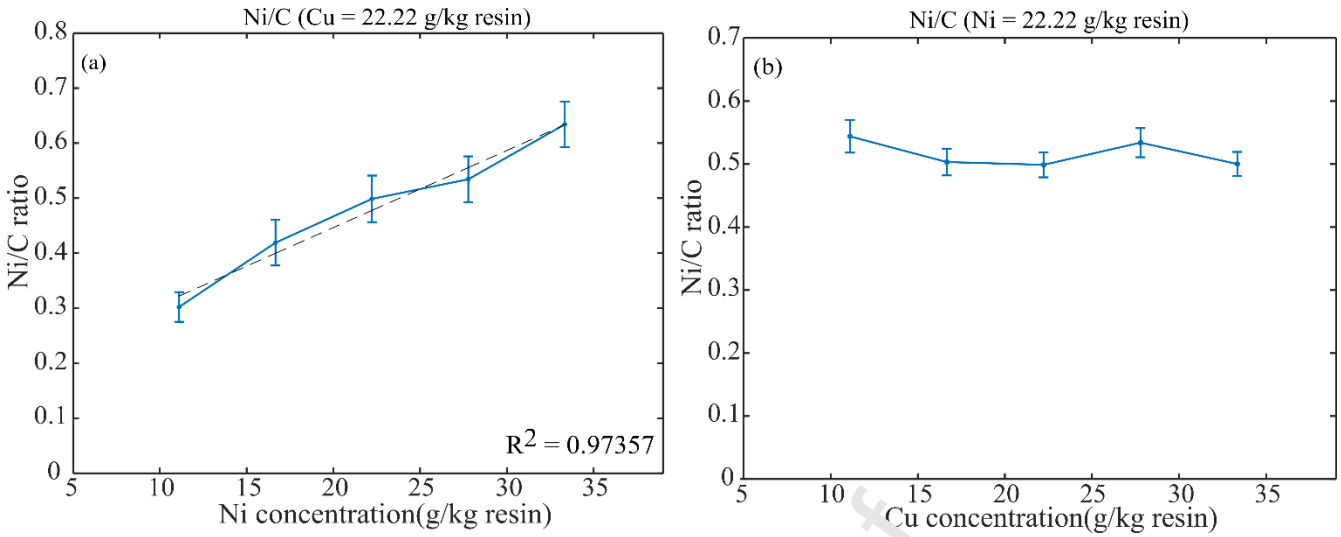

Figure 7. Relation between the intensity of Ni/C ratio and Ni concentration while Cu concentration is fixed (a), when Ni concentration is fixed and Cu is changing (b). Error bars represent standard error of the mean (SEM). The mean RSD of the measurements was 13.3% (a) and 12.5% (b).

Figure 7b shows the evolution of the Ni/C ratio at a constant Ni concentration when Cu concentration is increasing. As previously stated in the case of the copper ratio, the value of the Ni/C ratio, when the nickel concentration is constant, should not vary with the copper concentration. In this figure, the Ni/C ratio has some small variations about a constant value around 0.5, which are probably due to intrinsic LIBS fluctuation.

After observing the behaviour of both metals, it can be concluded that the presence of another metal does not affect the intensity of the measured metal ratio in either case.

3.3. Concentration prediction

After establishing the individual calibration curves of nickel and copper, it is necessary to test the accuracy of the predictions for bi-component samples. Binary mixture measurements were tested giving the following results.

Table 5. Predicted concentration of copper in bi-component samples with a fixed nickel concentration of 22.22 g/kg dry resin

Sample	Real Copper concentration in resin (g Cu/ kg dry resin)	Predicted concentration (g Cu/ kg dry resin)	Relative error (%)
1	11.111	11.979	7.81
2	16.667	15.308	8.15
3	22.222	23.222	4.50
4	27.778	27.248	1.91
5	33.333	33.683	1.05
		Mean error (%)	**4.69**

In Table 5, the real concentration of copper in presence of a nickel concentration of 22.22 g/kg resin is shown together with the predicted concentration based in the individual copper calibration curve. At first sight, the concentrations obtained by employing the calibration curve are quite precise, showing a mean prediction error of 4.69%.

Concerning the nickel concentration prediction, while copper concentration is set to 22.22 g/kg resin, Table 6 indicates the predicted nickel concentrations obtained from the individual nickel calibration curve applied to bi-component samples. The mean error of the prediction is 7.98%.

A trend towards reducing the relative error can be observed when the metal concentration increases, for both copper and nickel concentrations.

Table 6. Predicted concentration of nickel in bi-component samples with a fixed copper concentration of 22.22 g/kg dry resin.

Sample	Real Nickel concentration in resin (g Ni/ kg dry resin)	Predicted concentration (g Ni/ kg dry resin)	Relative error (%)
1	11.111	9.812	11.69
2	16.667	18.584	11.50
3	22.222	24.577	10.60
4	27.778	27.255	1.88
5	33.333	34.742	4.22
		Mean error (%)	**7.98**

Correlation figures 8 and 9 provide a visual impression of the accuracy of the concentration prediction. Real concentrations versus predicted concentrations are presented for copper and nickel predictions. It is noticeable that predicted and real concentrations are highly correlated (0.99 for Cu, 0.98 for Ni).

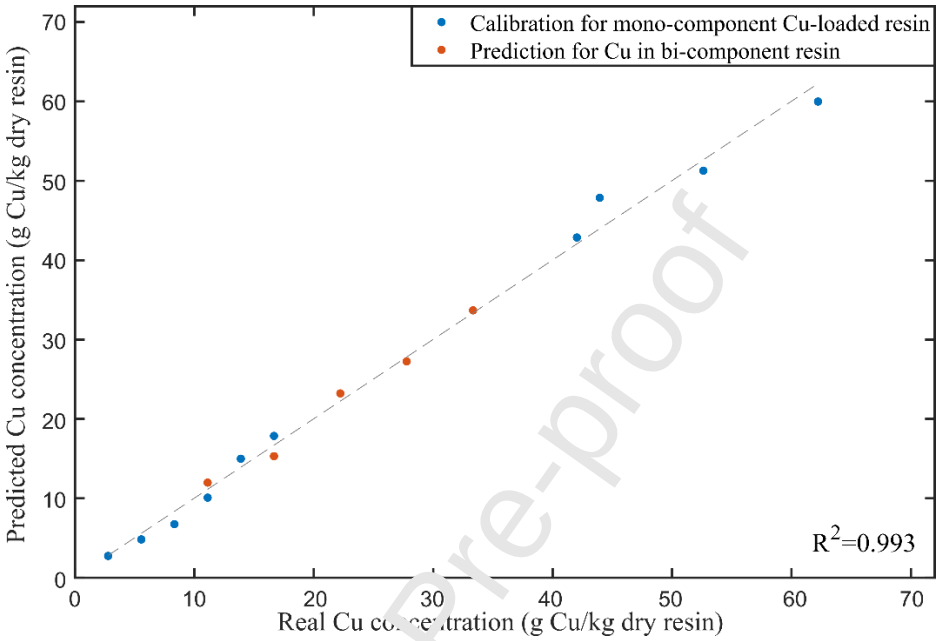

Figure 8. Correlation between real and predicted copper concentration.

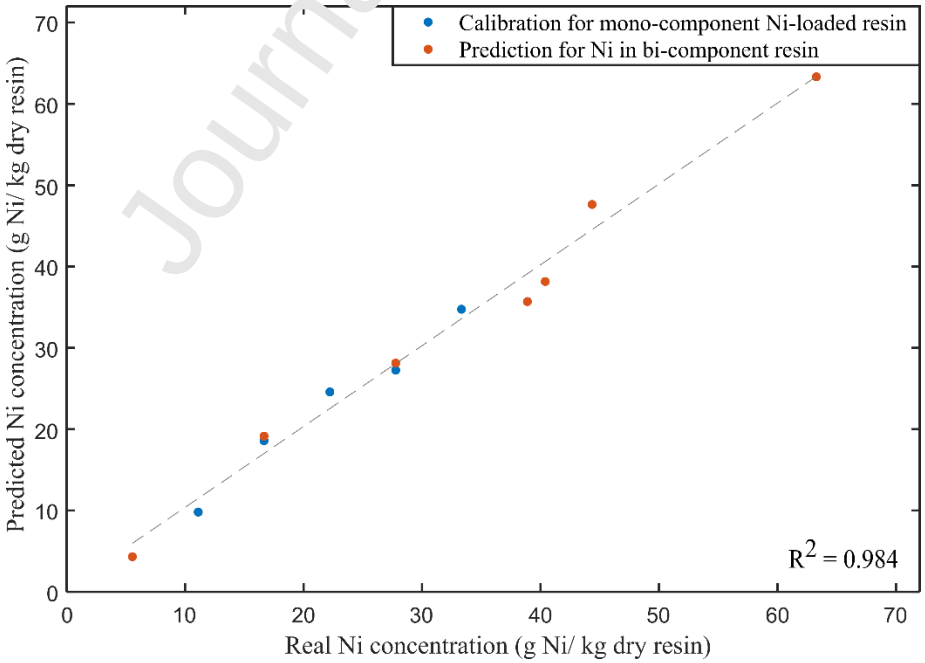

Figure 9. Correlation between real and predicted nickel concentration.

4. Conclusions

This work studies the suitability of LIBS for measuring nickel and copper concentration in selective chelating resins for metal recovery in wastewater applications. Individual nickel and copper calibration curves show a high correlation (0.99 and 0.98 respectively) between the real concentration of the metal adsorbed in the resin, and the ratio between the metal and carbon peak intensity signals. These results make the curves suitable for predicting concentrations in single-component-loaded resins. The influence of the presence of another metal adsorbed on the prediction of the concentration has also been studied. Nickel presence in copper concentration and vice versa does not affect how the intensity ratios depend on concentration. In terms of prediction accuracy, the mean relative error of copper concentration prediction was 4.69% and it was 7.98% for nickel prediction. The calibration curves for single-component resin provide a good concentration prediction based on intensity of Cu and Ni peaks when measuring bi-component charged chelating resin. The correlation between predicted concentration and the real concentration of copper and nickel was found to be good enough to perform analysis of unknown chelating resin samples with regression coefficients of 0.99 for copper and 0.98 for nickel concentration. Spent acids contains several additional metals in the composition such as aluminium, zinc or iron. Typically, iron peaks are usually very numerous on LIBS spectra; therefore, regarding the good prediction in bi-component resins, in further studies, the influence of these elements on copper and nickel signal will be studied by using chelating resins loaded with real spent acids. Future work will also focus on in-process dynamic studies of copper and nickel chelating resin adsorption, in order to examine the feasibility of monitoring a metal recovery process.

Acknowledgements

This research was developed in the framework of the projects TEC2016-76021-C2-2-R (AEI/FEDER, UE), PID2019-107270RB-C21/AEI/10.13039/501100011033, CTM2017-87740-R, RTI2018-093310-B-I00 and grant BES-2017-080076, all financed by the Spanish Ministry of Science, Innovation and Universities.

REFERENCES

1. Fu, F. & Wang, Q. Removal of heavy metal ions from wastewaters: A review. *J. Environ. Manage.* **92**, 407–418 (2011).

2. Ulloa, L., Bringas, E. & San-Román, M. F. Simultaneous separation of nickel and copper from sulfuric acid using chelating weak base resins. *J. Chem. Technol. Biotechnol.* **95**, 1906–1914 (2020).

3. Monier, M., Ayad, D. M., Wei, Y. & Sarhan, A. A. Preparation and characterization of magnetic chelating resin based on chitosan for adsorption of Cu(II), Co(II), and Ni(II) ions. *React. Funct. Polym.* **70**, 257–266 (2010).

4. San Román, M. F., Ortiz Gándara, I., Ibañez, R. & Ortiz, I. Hybrid membrane process for the recovery of major components (zinc, iron and HCl) from spent pickling effluents. *J. Memb. Sci.* **415**–**416**, 616–623 (2012).

5. San Román, M. F., Bringas, E., Ibañez, R. & Ortiz, I. Liquid membrane technology: Fundamentals and review of its applications. *J. Chem. Technol. Biotechnol.* **85**, 2–10 (2010).

6. Juang, R. S. & Shiau, R. C. Metal removal from aqueous solutions using

chitosan-enhanced membrane filtration. *J. Memb. Sci.* **165**, 159–167 (2000).

7. Bryson, A. W. & Dardis, K. A. Treatment of dilute metal effluents in an electrolytic precipitator. *Water SA* **6**, 85–87 (1980).

8. Akbal, F. & Camci, S. Copper, chromium and nickel removal from metal plating wastewater by electrocoagulation. *Desalination* **269**, 214–222 (2011).

9. Silva, J. E., Paiva, A. P., Soares, D., Labrincha, A. & Castro, F. Solvent extraction applied to the recovery of heavy metals from galvanic sludge. *J. Hazard. Mater.* **120**, 113–118 (2005).

10. Meunier, N. *et al.* Comparison between electrocoagulation and chemical precipitation for metals removal from acidic soil leachate. *J. Hazard. Mater.* **137**, 581–590 (2006).

11. Kang, S. Y., Lee, J. U., Moon, S. H. & Kim, K. W. Competitive adsorption characteristics of Co2+, Ni2+, and Cr3+ by IRN-77 cation exchange resin in synthesized wastewater. *Chemosphere* **56**, 141–147 (2004).

12. Kandah, M. I. & Meunier, J. L. Removal of nickel ions from water by multi-walled carbon nanotubes. *J. Hazard. Mater.* **146**, 283–288 (2007).

13. Monier, M., Ayad, D. M. & Sarhan, A. A. Adsorption of Cu(II), Hg(II), and Ni(II) ions by modified natural wool chelating fibers. *J. Hazard. Mater.* **176**, 348–355 (2010).

14. Wu, F. C., Tseng, R. L. & Juang, R. S. Kinetic modeling of liquid-phase adsorption of reactive dyes and metal ions on chitosan. *Water Res.* **35**, 613–618 (2001).

15. Zhou, L., Wang, Y., Liu, Z. & Huang, Q. Characteristics of equilibrium, kinetics studies for adsorption of Hg(II), Cu(II), and Ni(II) ions by thiourea-modified magnetic chitosan microspheres. *J. Hazard. Mater.* **161**, 995–1002 (2009).

16. Fernandes, S., Romão, I. S., Abreu, C. M. R., Quina, M. J. & Gando-Ferreira, L. M. Selective separation of Cr(III) and Fe(III) from liquid effluents using a chelating resin. *Water Sci. Technol.* **66**, 1968–1976 (2012).

17. Wang, C. C., Chen, C. Y. & Chang, C. Y. Synthesis of chelating resins with iminodiacetic acid and its wastewater treatment application. *J. Appl. Polym. Sci.* **84**, 1353–1362 (2002).

18. Mendes, F. D. & Martins, A. H. Selective sorption of nickel and cobalt from sulphate solutions using chelating resins. *Int. J. Miner. Process.* **74**, 359–371 (2004).

19. Littlejohn, P. & Vaughan, J. Selectivity of commercial and novel mixed functionality cation exchange resins in mildly acidic sulfate and mixed sulfate-chloride solution. *Hydrometallurgy* **121**–**124**, 90–99 (2012).

20. Sirola, K., Laatikainen, M., Lahtinen, M. & Paatero, E. Removal of copper and nickel from concentrated ZnSO4 solutions with silica-supported chelating adsorbents. *Sep. Purif. Technol.* **64**, 88–100 (2008).

21. Kołodyńska, D. The effect of the novel complexing agent in removal of heavy metal ions from waters and waste waters. *Chem. Eng. J.* **165**, 835–845 (2010).

22. Botelho Junior, A. B., Vicente, A. D. A., Espinosa, D. C. R. & Tenório, J. A. S. Recovery of metals by ion exchange process using chelating resin and sodium

dithionite. *J. Mater. Res. Technol.* **8**, 4464–4469 (2019).

23. Sengupta, A. K., Zhu, Y. & Hauze, D. Metal(II) Ion Binding onto Chelating Exchangers with Nitrogen Donor Atoms: Some New Observations and Related Implications. *Environ. Sci. Technol.* **25**, 481–488 (1991).

24. Spencer, J., Stevens, J., Perry, C. & Murphy, D. M. An EPR Investigation of Binding Environments by N-Donor Chelating Exchange Resins for Cu Extraction from Aqueous Media. *Inorg. Chem.* **57**, 10857–10866 (2018).

25. Qiu, X., Hu, H., Yang, J., Wang, C. & Cheng, Z. Removal of trace copper from simulated nickel electrolytes using a new chelating resin. *Hydrometallurgy* **180**, 121–131 (2018).

26. Cremers, David A. Radziemski, L. J. *Handbook of Laser-Induced Breakdown Spectroscopy*. (John Wiley & Sons, 2006).

27. Miziolek, Andrzej W., Vincenzo Palleschi, and I. S. (ed. . *Laser induced breakdown spectroscopy*. (Cambridge university press, 2006).

28. Galbács, G. A critical review of recent progress in analytical laser-induced breakdown spectroscopy. *Anal. Bioanal. Chem.* **407**, 7537–7562 (2017).

29. Ulloa, L., Martínez-Minchero, M., Bringas, E., Cobo, A. & San-Román, M. F. Split regeneration of chelating resins for the selective recovery of nickel and copper. *Sep. Purif. Technol.* **253**, 117516 (2020).

30. Purolite - Puromet MTS9600. Data sheet Puromet MTS9600. Available at: https://www.purolite.com/product/es/mts9600.

31. Wołowicz, A. & Hubicki, Z. The use of the chelating resin of a new generation Lewatit MonoPlus TP-220 with the bis-picolylamine functional groups in the removal of selected metal ions from acidic solutions. *Chem. Eng. J.* **197**, 493–508 (2012).

32. Hahn, D. W. & Omenetto, N. Laser-induced breakdown spectroscopy (LIBS), part II: Review of instrumental and methodological approaches to material analysis and applications to different fields. *Appl. Spectrosc.* **66**, 347–419 (2012).

CRediT authorship contribution statement

Marina Martínez-Minchero: Investigation, Formal analysis, Writing - Review & Editing

Laura Ulloa: Investigation, Formal analysis

Adolfo Cobo: Conceptualization, Supervision

Eugenio Bringas: Conceptualization, Supervision

M. Fresnedo San-Román: Supervision

José Miguel López-Higuera: Supervision

Highlights

- Generation of industrial wastewaters containing heavy metals is growing
- Chelating resins absorption is an effective treatment for heavy metals recovery
- LIBS offers the advantage of continuous monitoring the absorption process
- LIBS measurements of Cu and Ni on single and dual resins samples were performed
- Prediction of concentration is highly correlated with real values ($R^2 > 0.98$)